Virginia Commonwealth University
VCU Scholars Compass

Theses and Dissertations

Graduate School

2017

PO2 dependence of oxygen consumption in skeletal muscle of hypertensive and normotensive rats

Habiba Shah
Virginia Commonwealth University

Follow this and additional works at: https://scholarscompass.vcu.edu/etd

Part of the Alternative and Complementary Medicine Commons, Cellular and Molecular Physiology Commons, and the Laboratory and Basic Science Research Commons

© The Author

Downloaded from
https://scholarscompass.vcu.edu/etd/5000

This Thesis is brought to you for free and open access by the Graduate School at VCU Scholars Compass. It has been accepted for inclusion in Theses and Dissertations by an authorized administrator of VCU Scholars Compass. For more information, please contact libcompass@vcu.edu.

PO_2 DEPENDENCE OF OXYGEN CONSUMPTION IN SKELETAL MUSCLE OF HYPERTENSIVE AND NORMOTENSIVE RATS

A thesis submitted in partial fulfillment of the requirements for the degree of Master of Science at the Medical College of Virginia Campus, Virginia Commonwealth University

By

Habiba Shah
B.S., Virginia Commonwealth University, 2013

Director:
Roland N. Pittman, Ph.D.
Professor
Department of Physiology and Biophysics

Virginia Commonwealth University
Richmond, VA
August 2017

ACKNOWLEDGEMENTS

I would like to thank Dr. Roland N. Pittman for all his support throughout this entire process. He has been one of the kindest mentors I have had the pleasure of working with. Dr. Pittman always believed in me even when I felt like I could not move forward at times. He always gave me the wisest advice and truly made me feel like I could achieve anything despite any setbacks I faced. I will always be grateful to him.

A special thank you to Sami C. Dodhy for being one of the best teachers I was fortunate enough to be taught by. Sam always congratulated me on every successful experiment, and provided much needed moral support during the long hours dedicated to this project. Sam never left any of my questions unanswered, and was always patient to teach me the same procedure every possible way.

I would also like to thank Aleksander Golub for designing most of the equipment that I have used during this project. Although we never had a conversation, I remember him as a kind faced man sipping on tea conversing passionately (about technical things, I'm sure) with my fellow lab partner.

I would like to thank my lab partner Alex Liles. Alex, you have been a solid support system through all of this for me. I cannot thank you enough for taking time out of your day anytime I asked for help. Working on similar projects was helpful because I always had you to discuss my daily lab activities with. You are the best lab partner anyone could ask for!

Special thanks to members of the graduate advisory committee; Dr. Martin Mangino, and Dr. Qinglian Liu for giving me their time and allowing me to present my project to them.

Finally, I am forever indebted to my amazing, loving parents. Their support and love through all of this has made it all worthwhile.

Table of Contents

ACKNOWLEDGMENTS……………………………………………………………..…2

TABLE OF CONTENTS…………………………………………………………..…3

LIST OFTABLES……………………………………………………………..…......5

LIST OF FIGURES………………………………………………………….………6

ABSTRACT……………………………………………………………….……...…7

INTRODUCTION……………………………………………………………………...9

Cellular Need for Energy……………………………………….……..…....9

Blood and Microcirculation…….……………………………………….…………..9

PO_2 Dependence of Oxygen Consumption, VO_2 ………………..……………….12

Phosphorescence Quenching Microscopy…………………………………….……13

Spontaneously Hypertensive Rat (SHR): Hypertensive Animal Model……….……15

Human Essential Hypertension……………………………………………………..16

Purpose of Study……………………………………………………………………17

METHODS AND MATERIALS…………………………………………….………..…18

Animal models and Surgical Preparations………………………….……………..18

Femoral Vein Cannulation…………………………………………………………19

Tracheostomy…………………………………..……………….……….……20

Spinotrapezius Muscle Preparation………………………………...…………20

Phosphorescent Probe Application…………………….……………………..22

Phosphorescence Quenching Microscopy…………………..…………………..22

Photo-consumption of oxygen…………………………………….…………..….23

Tissue Compression……………………………………………………..………24

Phosphorescence Decay Curve Analysis……………………………..……………25

Analysis of Oxygen Consumption…………….…………………………………25

Statistics…………………………………………...……………………..26

RESULTS……………………………………………………….…………………27

Oxygen Disappearance Curves…………………………………...……….27

PO_2 Dependence of VO_2…………………………….………...... ………....…31

Blood Pressure Measurements…………………………………………......……32

VO_2 vs. PO_2 Plot - WKY Rat………………………...……...………………33

VO_2 vs. PO_2 Plot- SHR………………………………………….………..34

DISCUSSION………………………………………………………………………35

Major Findings……………………………………………………….….35

Oxygen Disappearance Curves……………………………………………..36

VO_2 vs. PO_2 Plots………………………………………….…………..37

Explanation for Increased V_{max} in SHRs…………………………….....…37

Oxidative Phosphorylation and Glycolysis………………………………..…..38

Limitations and Future Studies……………………………………………..39

Conclusion…………………………………………………………………40

REFERENCES…………………………………………………………….….41

APPENDIX…………………………………………………………………………43

WKY VO_2 vs. PO_2 Plots……………………………………………………43

SHR VO_2 vs. PO_2 Plots……………………………………………...……50

VITA………………………………………………………………………..55

LIST OF TABLES

Table 1. Hill values (V_{max}, P_{50}, and a) for Wistar-Kyoto and spontaneously hypertensive rats.

Table 2. Previously performed *in situ* study; Hill values (V_{max}, P_{50} and a) for Sprague-Dawley rats (Golub AS, Pittman RN, 2012).

Table 3. Mean systolic, diastolic, and heart rate measurements of Wistar-Kyoto and spontaneously hypertensive rats.

LIST OF FIGURES

Figure 1. Oxygen Dissociation Curve

Figure 2. Photograph of a spinotrapezius muscle prepared for PQM

Figure 3. Oxygen disappearance curve (WKY)

Figure 4. Oxygen disappearance curve (SHR)

Figure 5. VO_2 vs. PO_2 Plot (WKY)

Figure 6. VO_2 vs. PO_2 Plot (SHR)

PO$_2$ dependence of oxygen consumption in skeletal muscle of hypertensive and normotensive rats

By Habiba Shah, B.S
A thesis submitted in partial fulfillment of the requirements for the degree of Master of Science at the Medical College of Virginia Campus, Virginia Commonwealth University

Virginia Commonwealth University, 2017

Advisor: Roland N. Pittman, Ph.D.
Department of Physiology and Biophysics

Abstract

Human essential hypertension affects over 75 million people in the United States, and can lead to death due to its several serious health complications such as hypertension-related cardiovascular disease. The purpose of this research was to understand how hypertension could cause physiological changes to the microcirculation, specifically the PO$_2$ dependence of oxygen consumption (VO$_2$) in skeletal muscle of normotensive and hypertensive rats. The Spontaneously Hypertensive Rat (SHR) strain was used as the diseased model, and Wistar-Kyoto (WKY) rats were used as controls to conduct this study. The SHR strain develops hypertension between 5-6 weeks after birth with an average systolic blood pressure of 150 mmHg. By arresting blood flow using an objective-mounted inflatable airbag, PO$_2$ measurements were obtained along with an oxygen disappearance curve (ODC), which was used to calculate VO$_2$ over various ranges of physiological PO$_2$ values. PO$_2$ and VO$_2$ curves were analyzed based on Hill's equation to fit the data and describe the PO$_2$ dependence of VO$_2$. When compared to the

healthy Wistar-Kyoto rats, the SHRs exhibited a higher Vmax, or maximum rate of oxygen consumption. The average maximal rate of consumption by the hypertensive animal models could be a consequence of a “mitochondrial uncoupling” or some disconnect in the mitochondrial oxygen consumption and the normal corresponding ATP production. In conclusion, this project demonstrated that *in situ* muscle tissue from hypertensive and normotensive rats had a PO_2 dependence of oxygen consumption over a wide range of physiological PO_2 values and the hypertensive rats consumed oxygen at a higher maximal rate.

Introduction

Cellular Need for Energy

All cells in an organism require energy to perform various activities. This energy is made in the form of Adenosine Triphosphate (ATP). ATP is produced via oxidative phosphorylation and takes place inside the mitochondria of the cell. It is important for mitochondria to have a continuous supply of oxygen to provide for the synthesis of ATP to carry out cellular activities. The cardiovascular and respiratory systems are involved in the supply of oxygen to the body. The delivery of oxygen from the atmosphere and into the lungs, where it becomes oxygenated in the pulmonary capillaries and travels back to the left side of the heart is an example of the coordinated mechanisms of the cardiovascular and respiratory systems (Costanzo, 1998).

Blood and Microcirculation

Red blood cells account for approximately 40-45% of blood volume and contain hemoglobin, which plays a crucial role in the transport of oxygen through the vasculature. Hemoglobin is composed of four heme groups each containing an iron atom to which oxygen binds. Once oxygen binds to hemoglobin, it is carried in this bound state until it is released and can diffuse out of the red blood cells and into the plasma, where it diffuses from the capillaries and into the surrounding tissues. The relationship between oxygen and hemoglobin is best understood through the oxygen dissociation (or saturation) curve (Figure 1). Certain physiological changes (e.g., changes in temperature, pH, PCO_2) can cause a shift in the dissociation curve to adjust the availability of oxygen to tissues. With an increase in temperature due to strenuous activity, the curve can shift to the right to decrease the affinity of hemoglobin for oxygen, thus releasing oxygen more easily (Pittman, 2011). When the partial pressure of oxygen (PO_2) in the blood is high, hemoglobin binds oxygen to form oxyhemoglobin. Once a single oxygen molecule has been bound, hemoglobin's affinity for the remaining three molecules increases, resulting in the sigmoidal shape of the curve. When PO_2 is low, oxyhemoglobin releases oxygen into the blood (Wells, 2009).

All cells are surrounded by the interstitial fluid (ISF) and the circulatory system is responsible for constantly replenishing the ISF with its normal chemical environment from the arterial blood. The ISF, however, does not constitute a large proportion of fluid volume and can only be considered a relatively small reservoir of fluid (Pittman, 2011). The difference in the partial pressure of oxygen within the microvessels and tissues allows oxygen to move out of the capillaries and into the ISF. Once oxygen diffuses into the ISF, it can then move into cells and undergoes consumption in cellular respiration to produce ATP (Pishchany G, 2012).

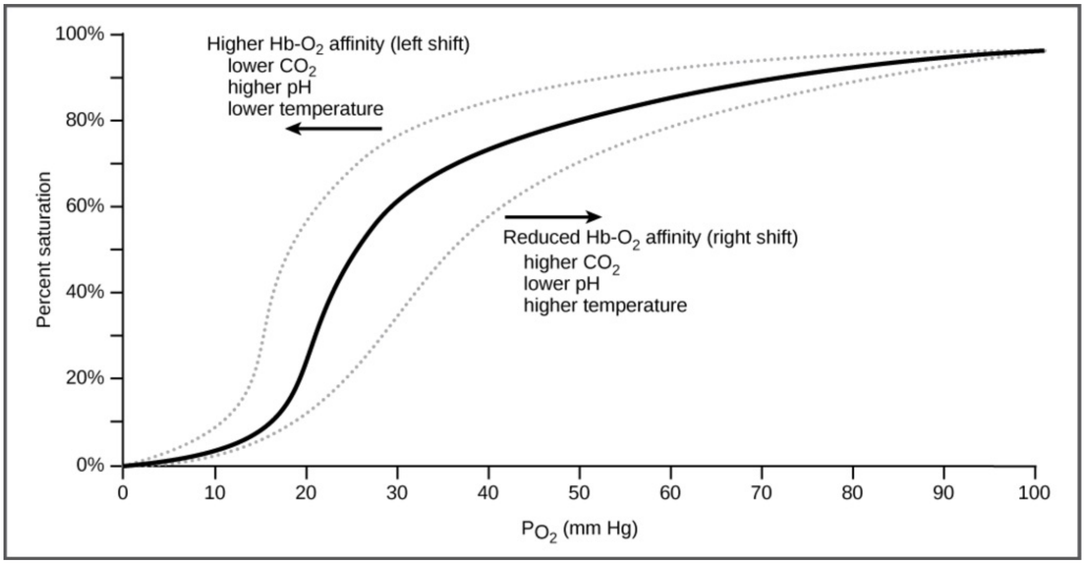

Figure 1. Oxygen dissociation curve

The production of ATP begins with the breakdown of carbohydrates once they are consumed. During glycolysis, glucose molecules are metabolized to produce carbon dioxide, water and ATP. Each glucose molecule that is broken down produces two pyruvate molecules. These pyruvate molecules then enter the Tri-Carboxylic Acid, the TCA or Krebs Cycle. This process of cellular respiration continues with the electron transport chain (ETC) in the mitochondria. The ETC involves the transfer of electrons from one carrier protein to the next, which are all embedded in the inner mitochondrial membrane. With the transfer of electrons, a proton gradient forms across the mitochondrial membrane and is used to produce ATP via oxidative phosphorylation. The electron transport chain terminates with oxygen accepting the electron. This pathway of cellular respiration occurs under aerobic conditions. Under anaerobic conditions, a different process known as fermentation occurs, which produces lactate and a lower yield of ATP.

PO_2 Dependence of Oxygen Consumption, VO_2

Living cells are comprised of several organelles, each of which performs its own functions to keep an organism's system in balance, so-called homeostasis. The mitochondria of the cell are considered the powerhouse because they are responsible for producing ATP. The majority of the oxygen is consumed by the mitochondria in order to keep a balanced output of ATP. Mitochondria can sustain a normal amount of oxygen consumption until the point where oxygen levels drop below a "critical" value ($PO_2 = 1$ mmHg) (Wilson, 1985**).** Since normal PO_2 levels are much higher than the critical value, it could be suggested that the mitochondrial consumption of oxygen remains unaltered throughout the normal physiological range of PO_2. Several *in vitro* studies that have measured oxygen consumption rates in mitochondrial suspensions have supported this idea (Wilson, 1988). However, *in vivo* studies have shown that mitochondrial oxidative phosphorylation could be dependent on varying oxygen concentrations over a much wider range. These studies suggest that oxygen consumption varies under different ranges of physiological PO_2 levels and that mitochondria do not function in an "all-or-nothing manner" (Golub & Pittman, 2012).

In order to understand the relationship between oxygen consumption, VO_2, and oxygen tension (or partial pressure), PO_2, it is instructive to plot the two together and interpret the results based on an empirical equation, Hill's equation, that looks similar to that describing Michaelis-Menten kinetics. The maximum rate of consumption (V_{max}) and the half-maximal rate (at $PO_2 = P_{50}$) can be calculated using the following equation:

(1) $VO_2 = V_{max}\, PO_2^a \,/\, [P_{50}^a + PO_2^a]$ (where a is Hill's coefficient).

Phosphorescence Quenching Microscopy

The method used in this study to measure oxygen levels (PO_2) involves the use of phosphorescence quenching microscopy (PQM) to evaluate oxygen consumption in rat spinotrapezius muscle. The PQM technique measures tissue VO_2 based on the analysis of an oxygen disappearance curve (ODC). The ODC is obtained by compression of the microcirculation and tissue with an objective-mounted airbag on the microscope. PQM uses the excitation of a phosphor probe molecule from its ground state to an excited state with the use of a brief flash from a laser beam. The probe can absorb some of the excitation light to produce excited triplet states, which can subsequently be quenched by oxygen (collisional quenching). It is therefore important to note that a fraction of oxygen is consumed during each excitation cycle. This is known as photo-consumption of oxygen. For continuous PO_2 measurements, the laser is flashed repeatedly at selected time intervals. The signal is localized based on the illumination area, amount of probe distributed on the muscle, and the penetration depth of the light. (Golub and Pittman, 2010).

To collect the ODC under conditions in which the tissue is isolated from atmospheric oxygen, the tissue is covered with a gas barrier film once the probe is applied. Furthermore, to reduce the contribution of hemoglobin to the ODC, the PQM method uses rapid onset of pressure in the objective-mounted inflatable bag, which immediately arrests the circulation and extrudes blood from the microvessels. This process allows the ODC to be independent of hemoglobin contribution (Golub and Pittman, 2010). To prevent the probe from penetrating into the parenchymal cells, it is bound to albumin, which is too large to enter cells; any albumin-bound probe, which enters the vasculature, is rapidly washed away by blood flow. The phosphorescent probe is topically applied to the thin spinotrapezius muscle. After application, an equilibration time of approximately 50-60 minutes is set for the probe's diffusion into the interstitial space (Nugent et al, 2015). When PO_2 measurements are obtained from the muscle, a "stop-flow" approach is used to find the VO_2 based on the subsequent rate of decrease in oxygen tension. Even when blood flow is arrested, the tissue continues to consume dissolved oxygen and the PO_2 falls almost linearly until it reaches approximately 10 mmHg. PO_2 calculated in this way is based on the Stern-Volmer equation.

(2)
$$\boldsymbol{k = k_0 + k_q PO_2}$$

In this equation, k is the rate of phosphorescence decay, k_q is the quenching coefficient, and k_0 is the decay rate at $PO_2 = 0$. They are also constants according to calibration studies (Golub et al, 2016).

Just after the phosphor is excited, the phosphorescence decays within an approximately exponential time course:

(3)
$$\boldsymbol{I_{phos}(t) = I_{phos}(0)\, e^{-kt}}$$

In the equation above, $I_{phos}(t)$ is the intensity of phosphorescent light emission, k is the phosphorescence (exponential) decay rate, and $I_{phos}\,(0)$ is the intensity of the phosphorescence at $t=0$.

Spontaneously Hypertensive Rat (SHR): Hypertensive Animal Model

This study involved the use and comparison of male spontaneously hypertensive rats (SHR) to normotensive Wistar-Kyoto (WKY) control rats. In an effort to study human hypertension using animal models, Professor Kozo Okamoto and his colleagues in Kyoto, Japan developed the SHR strain. They measured the blood pressure of Wistar colony rats and picked those with elevated blood pressures, 150 mmHg, to mate and breed (Okamoto & Aoki, 1963). For experimental purposes, the WKY strain serves as a control for the SHR strain.

Hypertension develops in the SHR rats within the first five weeks of development. They remain normotensive prior to developing hypertension with a systolic blood pressure of approximately 150 mmHg. In the earlier stages of life, SHR rats manifest an increased cardiac output and normal total peripheral resistance. However, later on in life cardiac output tends to normalize, whereas the total peripheral resistance increases. A similar hemodynamic pattern is seen in humans with essential (idiopathic) hypertension as well.

The prolonged exposure to hypertension in SHR rats causes them to exhibit similar health complications as humans with essential hypertension, including myocardial infarction, cerebral lesions, renal damage, etc. The onset of hypertension is more severe in the male strain compared to female rats. Due to these complications, the average lifespan of the male SHR strain is around 18 months relative to the 24-month lifespan of the WKY strain (Okamoto & Aoki, 1963).

Human Essential Hypertension

Human essential hypertension affects over 75 million people in the United States, potentially leading to major cardiovascular complications including ventricular hypertrophy and dilation. These serious complications are often the cause of congestive heart failure, stroke, and renal damage. This multifactorial and polygenic disease can be promoted by genetic and/or environmental factors. Several clinical and experimental studies have suggested that the underlying mechanisms of hypertension include an increased activity of the sympathetic nervous system, over-active renin-angiotensin-aldosterone system, and cardiac hypertrophy. (Wang et al, 2013).

It is important to note the similarities between the SHR rats and humans with essential hypertension, since the symptoms of hypertension, apart from high blood pressure and elevated peripheral resistance, are initially not evident in both humans and rats.

Purpose of Study

The purpose of this project was to study the PO_2 dependence of oxygen consumption in normotensive and hypertensive rat skeletal muscle. Previous *in vivo* studies have demonstrated that mitochondrial oxygen consumption rate is dependent on PO_2 values over a wider range than previously proposed (Golub and Pittman, 2012). To further strengthen this investigation, this project sought to determine if PO_2 values and dependence is altered in a diseased animal.

The spontaneously hypertensive rat (SHR) is a model used for human essential hypertension. By analyzing the oxygen disappearance curve, we were able to determine if indeed there is a difference in mitochondrial oxygen consumption of normotensive and hypertensive rats. The oxygen disappearance curves were obtained after blood flow was halted using phosphorescence-quenching microscopy.

Materials and Methods

Animal Models

In this experiment, Wistar-Kyoto (WKY) rats were used as the control group. The Spontaneously Hypertensive Rat (SHR) strain was used as the diseased model. The average weight of the WKY controls was 271 grams ± 9.3; average weight of the SHRs was 321 grams ± 15.7 and they were age-matched so that all animals were between 12-14 weeks old. All animals used in this experiment were housed in a vivarium under controlled conditions (40-60% humidity, 20-23 ºC, 12:12 hours light/dark cycle). They had access to food and water until the time of the experiment under the supervision of a certified animal technician. Both the WKY controls, and the SHRs were subjected to the same experimental protocol. Using a ketamine/ acepromazine (75/ 2.5/ mg/ kg) mixture anesthetic the animal was anesthetized in the intraperitoneal space with a B-D 27G ½ Precision Glide Needle. Once the animal was sedated, it was shaved along the neck, spine, and lower inguinal regions using clippers. Nair depilatory cream was used to remove the remaining unwanted hair in those regions (Nair, Church and Dwight Co., Inc., Ewing, NJ). The rat was transferred onto a heated homoeothermic platform (Golub & Pittman, 2003) set at 37°C to maintain body temperature. Using the CODA Monitor (Computerized, Non-Invasive Blood Pressure Monitor for Mice and Rats), the animal's blood pressure and heart rate were monitored. This method involves placing an occlusion tail-cuff, which upon inflation impedes blood flow. A Volume Pressure Recording (VPR) sensor serves as a second cuff, which measures the returning blood flow. As the occlusion cuff deflates, the VPR sensor cuff measures the swelling of the tail due to arterial pulsations. The very first indication of tail swelling measures the systolic blood pressure. The diastolic blood pressure is measured as the swelling starts to cease. The CODA Monitor is able to provide accurate blood pressure readings in a non-invasive manner, which avoids further surgical preparation (CODA System, Kent Scientific, Torrington, CT).

Femoral Vein Cannulation

The right femoral vein was cannulated using a cannula of polyethylene tubing (PE 90) for administration of intravenous anesthetic. The cannula was connected to a 5 mL syringe containing Alfaxan (Jurox Inc., Kansas City, MO, alfaxalone 10 mg/mL) and a 10 mL syringe with heparinized phosphate-buffered saline (H-PBS). A continuous intravenous infusion of Alfaxan was maintained (at 0.01 mg/ mL x min) for the duration of the experiment.

To perform the femoral vein cannulation, an incision was made along the right inguinal crease. The right femoral vein was isolated and the distal end was tied off to arrest blood flow. The proximal end of the vein was tightened off around the cannula to secure its insertion during the experiment.

Throughout the experiment and immediately after cannulation, the animal’s toe pinch reflex and heart rate were monitored to ensure the appropriate infusion rate of Alfaxan. The cannula was taped to the animal’s leg to keep it secured.

Tracheostomy

A tracheostomy was performed to insure a patent airway. An incision was made in the anterior neck and the subcutaneous tissue was dissected to expose the trachea. The trachea was intubated with polyethylene tubing (PE 240, Clay Adams, Parsippany, NJ).

Spinotrapezius Muscle Preparation

The spinotrapezius muscle was isolated by making a dorsal midline incision along the spine and extending superiorly to the scapula. Using a pair of Metzenbaum scissors under the muscle, the overlying connective tissue was carefully dissected in order to prevent trauma and excess bleeding of the spinotrapezius muscle. During dissection a low-temperature cautery device was used to stop any bleeding that occurred. The muscle was maintained moist by application of phosphate buffered saline (PBS) as needed. Once the muscle was separated from the underlying connective tissue, it was flattened for viewing. Silk sutures (size = 6-0) were placed around the border of the muscle at 2 cm intervals. The animal was transferred onto a thermostable Plexiglas viewing platform (Golub & Pittman, 2003) where the excised muscle was mounted ventral side up. The muscle was flattened onto the platform by gently pulling on the silk sutures at the lateral margins so as not to stretch the muscle and attaching them to the pedestal.

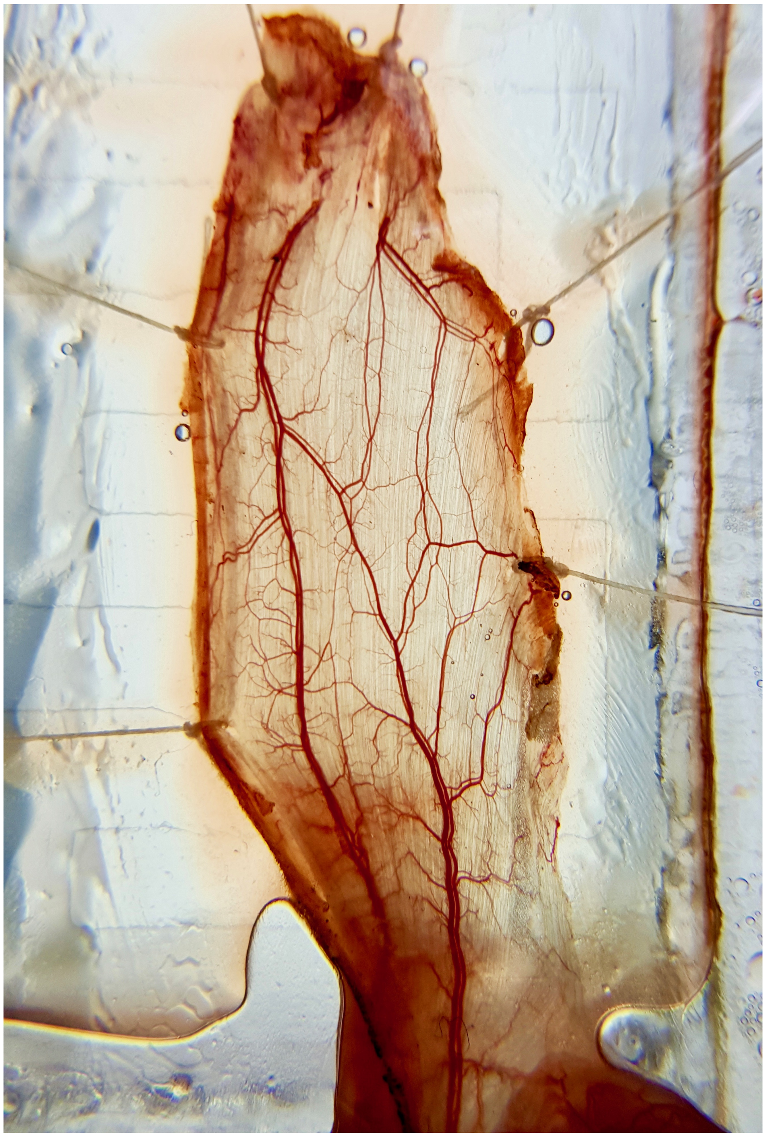

Figure 2. Photograph of a spinotrapezius muscle prepared for phosphorescence quenching microscopy.

Phosphorescent Probe Application

Once the muscle was secured to the heated pedestal (Golub & Pittman, 2003), 2 mL of the phosphorescent oxygen probe [Pd-meso-tetra-(4-carboxyphenyl) porphyrin {Oxygen Enterprises, Philadelphia, PA}] was topically applied to the muscle. Previous studies have shown that the probe was uniformly distributed throughout the interstitial space after a diffusion time of ~50 minutes. Since the probe is bound to serum albumin it can be assumed that it did not penetrate the muscle fibers because albumin is too large to pass through the cell membrane. Furthermore, the continuous blood flow in the muscle would "wash out" any probe that might have entered the microvessels. Hence, it was assumed that measurements of PO_2 taken after the probe was excited were indeed coming from the interstitial space. After application of the probe, a piece filter paper was placed on top of the muscle and the entire muscle was covered with plastic film (Krehalon, CB-100; Krehalon Limited, Japan) to minimize gas exchange with the atmosphere.

Phosphorescence Quenching Microscopy (PQM)

The thermostable Plexiglas viewing pedestal (Golub & Pittman, 2003) was placed on the stage of an Axioplan-2 microscope (Zeiss, Germany). A well-perfused site was chosen with the help of a video camera connected to the microscope.

Once a well-perfused site on the muscle was chosen, it was important to ensure that the pneumatic compressions resulted in extrusion of blood from the microvessels at that particular site.

The phosphorescent probe was excited using a laser, which was flashed at a rate of 1 Hz. The resulting phosphorescence passed through a dichroic mirror and was detected by a photomultiplier tube (PMT). The signal from the PMT was amplified and transmitted to an analog-to-digital converter, which helped produced a digitized phosphorescence decay curve. The phosphorescence decay curves were analyzed to produce one PO_2 value for each decay curve using the National Instruments platform software.

Photo-consumption of Oxygen

When the laser excited the phosphor probe, the excited phosphor returned to the ground state by emitting a photon or through a transfer of energy to nearby oxygen molecules. Interaction of the excited phosphor with an oxygen molecule results in singlet oxygen, a highly reactive form of oxygen, which interacts with nearby organic molecules. Thus, some oxygen is "consumed" by the method itself. The magnitude of the photo-consumption is directly proportional to tissue PO_2. The reduction in PO_2 is accounted for by calculating a proportionality coefficient (*K*) that yields the rate of photo-consumption. To calculate *K*, PO_2 is measured at two different excitation frequencies using a 5 sec x 15 sec high/low pressure cycling method (Nugent et al, 2015). A series of 5 sec compressions followed by 15 seconds without compression (recovery) for a total of 100 seconds measures the PO_2 between high and low frequencies. By comparing those PO_2 changes, the photo-consumption coefficient is calculated using the following formula:

(4) $$K = [(dP_n/dn)_1 - (dP_n/dn)_2]/[(FP_0)_2 - (FP_0)_1]$$

In this equation, dP_n/dn is the rate of oxygen disappearance per flash at a given frequency (denoted by 1 or 2, representing the high or low frequency, respectively). F is the flash rate per measurement. P_0 is the steady-state PO_2 at a given flash rate before the tissue is compressed.

Tissue Compression

To stop blood flow in the muscle, an airbag attached to the objective of the microscope was rapidly inflated, arresting blood flow in the spinotrapezius muscle. The airbag was inflated to approximately 150 mmHg (at <1s). With the aid of a video camera, the tissue could be visualized as the blood flow ceased, and red blood cells were extruded from the compressed portion of the muscle. With the compression of the muscle, a fall in PO_2 was observed. This decrease was caused by consumption of dissolved oxygen by the tissue. A total of five well-perfused sites were chosen per experiment. This was determined by choosing sites on the muscle where blood flow had a continuous, rapid movement. The sites chosen on the muscle were selected to avoid any interference with surrounding major blood vessels.

Prior to the tissue compressions, a baseline PO_2 measurement was made for each site. Following inflation of the airbag the PO_2 was measured for one minute to obtain a complete oxygen disappearance curve. After each compression, the tissue was allowed to rest for five minutes between measurements to restore blood flow to the site.

Phosphorescence Decay Curve Analysis

The phosphorescence decay curves were analyzed using a nonlinear fitting program based on the rectangular $P_{ISF}O_2$ distribution model (Golub et al., 1997). With the help of the fitting program, a continuous line fit was obtained for the decay curves to calculate the rate of phosphorescence decay. The following fitting equation was used:

$$\textbf{(5)} \qquad \boldsymbol{I(t) = I_0 \exp[-(K_0 + K_q M)t]\sinh(K_q \delta t)/K_q \delta t + B}$$

In this equation, t is time in s from the start of the decay, $I(t)$ is the phosphorescence decay curve in volts, I_0 is the phosphorescence signal's magnitude at t = 0. K_0 and K_q serve as constants determined by calibration experiments (Golub and Pittman, 2016) where $K_0 = 1.53 \times 10^{-4}\ \mu s^{-1}$ and $K_q = 4.3 \times 10^{-4}\ \mu s^{-1}\ mmHg^{-1}$. M is the average PO_2 (mmHg) in the measurement region, δ (mmHg) is half-width of the uniform PO_2 distribution, and B (volts) is the baseline offset of the amplifier.

Oxygen Consumption Analysis

An oxygen disappearance curve (ODC) was created for each site following a drop in the PO_2 due to tissue compression. The drop in PO_2 was due to several factors. The consumption of dissolved oxygen by the tissue as part of cellular respiration contributed to the drop in PO_2. Furthermore, when the laser beam excited the probe, the resulting singlet oxygen reacted with nearby organic molecules. This accounted for consumption of oxygen by the method itself.

The rate of oxygen consumption (V_n) was calculated using the oxygen disappearance curves at a given PO_2. The relationship between PO_2 and V_n is described by the following formula:

$$\frac{dP_n}{dn} = -V_n - KP_n + Z(P_n - P_n) \tag{6}$$

In this formula dP_n / dn is the rate of oxygen disappearance per flash. Z is the coefficient related to inward diffusion of oxygen into the excitation region, K is the coefficient related to consumption by the PQM method. The tissue had passive inward oxygen diffusion, however, the area of tissue that was excited was large enough so that the contribution of oxygen diffusion into the excited region had a negligible effect on the average PO_2 in that region.

Statistics

All values in the tables are mean ± SE (N). An unpaired t-test was performed to test for significance between results for the WKY and SHR groups; significance was assigned at $p<0.05$.

Results

To determine whether there was a difference in oxygen dependence of oxygen consumption between hypertensive (SHR) and normotensive (WKY) animal models. The data collected was based on the “flow arrest” approach described previously.

Oxygen Disappearance Curves

Once the spinotrapezius muscle was prepared and mounted on the animal platform, oxygen disappearance curves were obtained using flash number and PO_2 data. Using Equation 4., these curves were corrected for consumption by the PQM method. The first 10 seconds served as a baseline PO_2 value prior to compression of the muscle. The airbag was inflated after 10 seconds and the ODC was created based on a PO_2 decrease. Figures 2 and 3 are a representation of the oxygen disappearance curves collected from the Wistar-Kyoto and spontaneously hypertensive rats, respectively.

Oxygen Disappearance Curve - WKY Rat

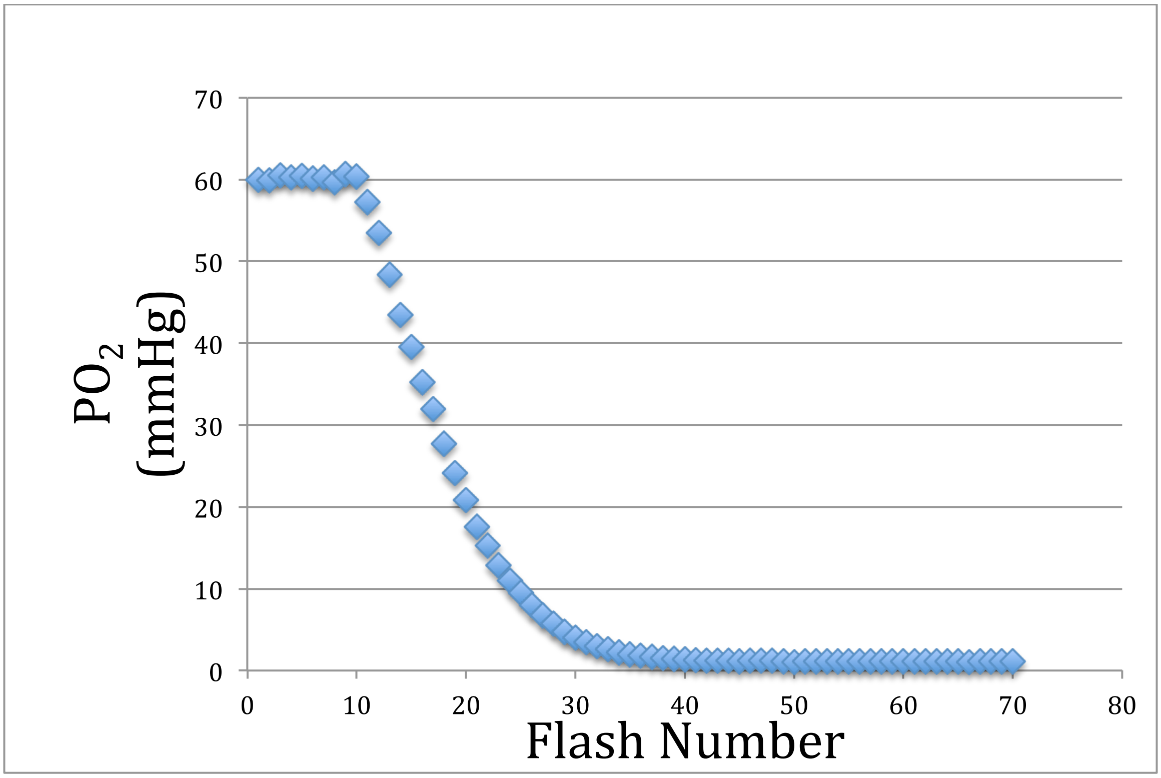

Figure 2. The figure above is an example of an oxygen disappearance curve (ODC) obtained from the spinotrapezius muscle of a Wistar-Kyoto control rat using PQM. The rate of the flash was 1 Hz, resulting in one PO_2 value each second.

Oxygen Disappearance Curve- SHR

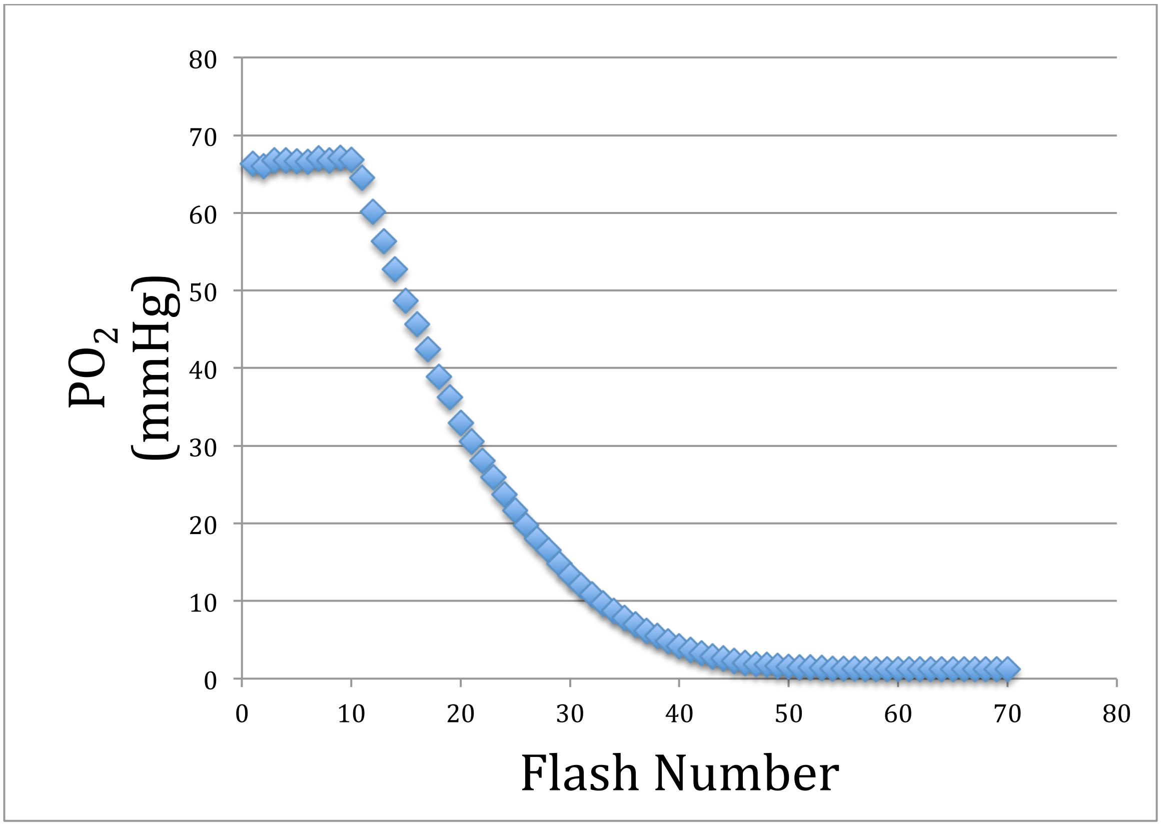

Figure 3. The figure above is an example of an oxygen disappearance curve (ODC) obtained from the spinotrapezius muscle of a spontaneously Hypertensive rat. The rate of the flash was 1 Hz, resulting in one PO_2 value each second.

	V_{max}(nl O_2/ cm^3*s))	P_{50} (mmHg)	a
WKY (12)	148.9 ± 14.1	8.9± 0.8	1.8± 0.1
SHR (14)	169.8± 17.7	22.3± 3.6	1.4±0.1

Table 1. The table above shows the best-fit values for V_{max}, P_{50}, and a (mean ± SE) for Wistar-Kyoto (WKY) control and Spontaneously Hypertensive rats (SHR). The number in parenthesis next to the strain indicates the amount of sites used per model.

	V_{max}(nl O_2/ cm^3*s))	P_{50} (mmHg)	a
Sprague-Dawley (34)	120.9± 7.7	11.1± 0.9	2.0± 0.1

Table 2. The table above shows the best-fit values for V_{max}, P_{50}, and a (mean ± SE for Sprague-Dawley rats as part of the previous *in situ* study performed (Golub AS, Pittman RN, 2012).

PO_2 Dependence of VO_2

Using the oxygen disappearance curves, VO_2 for each PO_2 value were calculated. VO_2 vs. PO_2 plots were created and fit with Hill's equation (Equation 7).

(7)

$$\boldsymbol{VO_2 = \frac{Vmax \times P_n^a}{P_{50}^a + P_n^a}}$$

In this equation, P_n is the PO_2 at a given flash number in the oxygen disappearance curve and VO_2. V_{max} is the maximal rate of respiration, a is the Hill's coefficient, and P_{50} is the half-maximal PO_2.

Once the VO_2 vs. PO_2 plots were fit with Hill's equation, V_{max}, P_{50} (K_m) and a were obtained. The mean V_{max} for the WKY control rats was 148.9 ± 14.1(SE) nl O_2 / (cm^3 *s). The mean P_{50} was 8.9±0.8 (SE) mmHg. The mean V_{max} of the SHR was 169.8 ±17.7 (SE) nl O_2 / (cm^3 *s).

	Systolic (mmHg)	Diastolic (mmHg)	Heart Rate (bpm)
WKY	114.3± 2.1	87.2± 7.8	373.2± 14.5
SHR	156.8± 4.1	120.7± 3.8	407.3± 22.9

Table 3. The table above includes the mean systolic, diastolic, and heart rate ($\pm SE$) of the Wistar-Kyoto controls and spontaneously hypertensive rat models.

VO_2 vs. PO_2 Plot - WKY Rat

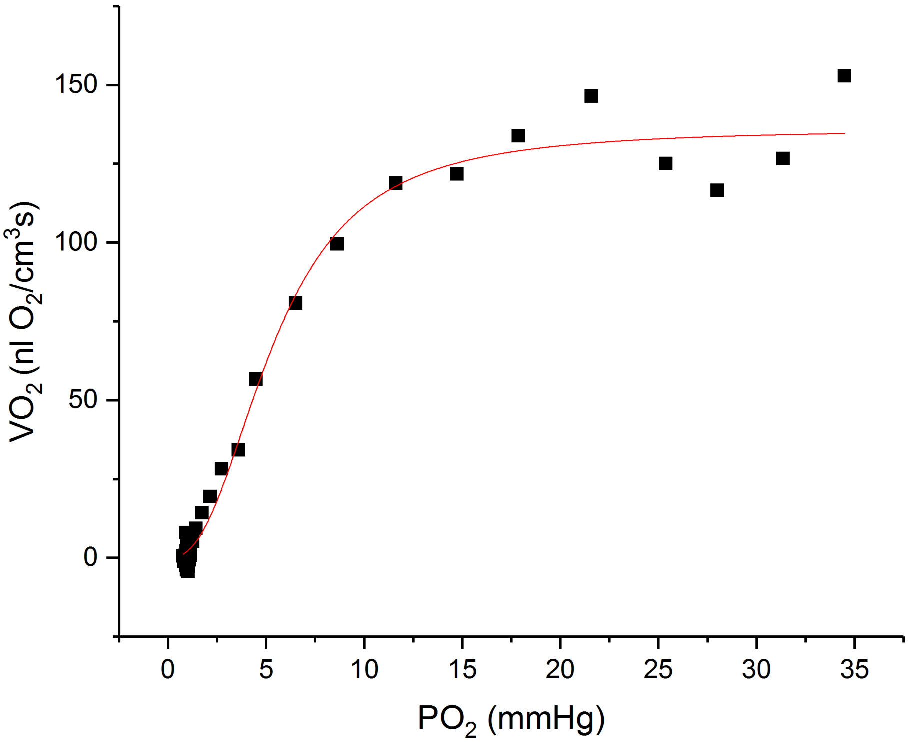

Figure 4. This is an example of a VO_2 vs. PO_2 plot used to measure the oxygen dependence of respiration in the spinotrapezius muscle of a Wistar-Kyoto rat. This plot is a representation of measurements obtained from a single site on the muscle. The Hill's parameters calculated include V_{max} (148.9 ± 14.1), P50 (8.9± 0.8), *a* (1.8±0.1).

VO_2 vs. PO_2 Plot- SHR

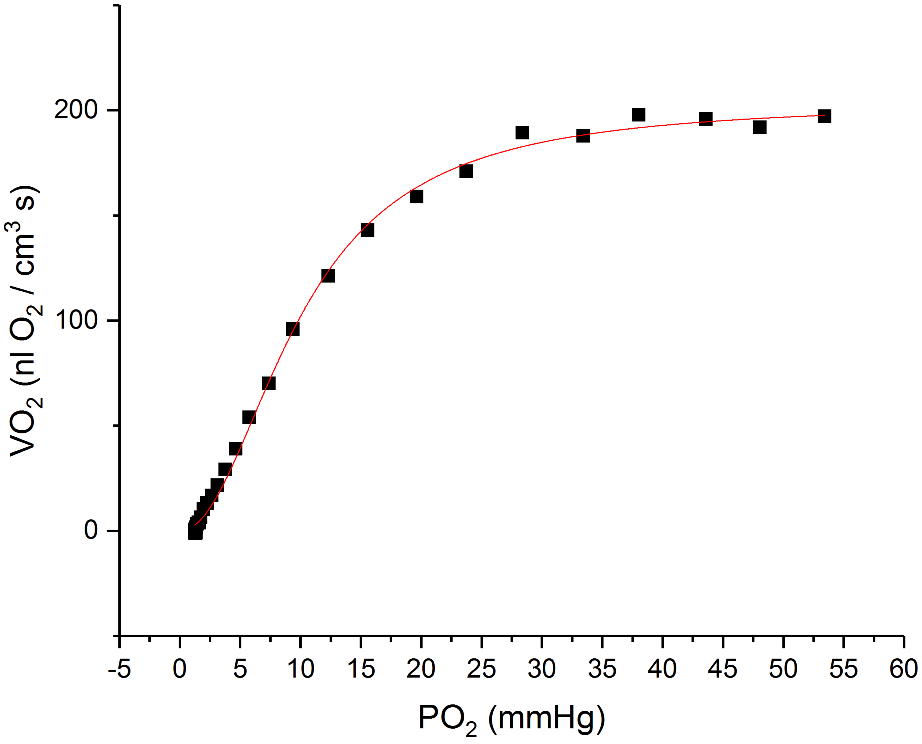

Figure 5. This is an example of a VO_2 vs. PO_2 plot used to measure the oxygen dependence of respiration in the spinotrapezius muscle of a spontaneously hypertensive rat. This plot is a representation of measurements obtained from a single site on the muscle. The Hill's parameters calculated include V_{max} (169.8 ± 17.7), P_{50} (22.3 ± 3.6) and *a* (1.4 ± 0.1)

Discussion

Major Findings

The major finding of this project was that the maximal rate of oxygen consumption, V_{max} in the spinotrapezius muscle of the rat with the use of phosphorescence quenching microscopy was higher in the spontaneously hypertensive Rat compared to the Wistar-Kyoto control rats: SHR Vmax169.8 ± 17.7 nl O_2 / (cm^3* s) and WKY, Vmax = 148.9 ± 14.1 nl O_2 / (cm^3 *s).

These values indicate that the hypertensive rats have an elevated rate of oxygen consumption in resting striated muscle when PO_2 is not limiting oxygen consumption. The PO_2 for half-maximal values of oxygen consumption, P_{50}, were different between the two strains (WKY, P_{50} = 8.9 ± 0.8 mmHg and SHR, P_{50} = 22.3 ± 3.6 mmHg).

This project focused on using a wide range of physiological PO_2 values to measure PO_2 dependence of oxygen consumption in both the WKY and SHR models. This project can be compared to previous studies that focused on mitochondrial oxygen consumption at a constant rate regardless of oxygen tension up until the PO_2 values fell below a “critical value” of approximately 1 mmHg (Wilson, 1985). Previous studies performed on the spinotrapezius muscle of male Sprague-Dawley rats have suggested that PO_2 values over a wider range correlate to oxygen consumption with a higher sensitivity (Golub & Pittman, 2003). The range is consistently wide in the muscles of the spontaneously hypertensive rats and Wistar-Kyoto control rats

Oxygen Disappearance Curves

The oxygen disappearance curves obtained from the SHR and WKY animal models display similar behavior observed in the spinotrapezius muscle from Sprague-Dawley rats in terms of oxygen consumption over time (Golub & Pittman, 2012). The first 10 seconds account for the baseline PO_2 before the airbag was inflated, thereby compressing the tissue. The baseline PO_2 is a representation of the amount of oxygen maintained in equilibrium in the interstitial fluid by the flow of oxygenated blood in the microcirculation and tissue consumption. The Spontaneously Hypertensive rats had a higher baseline PO_2 compared to the Wistar-Kyoto control rats. The equilibrium was disturbed when the airbag was inflated and the muscle was compressed at 10 seconds. PO_2 began to decrease in the compressed portion of the muscle, because red blood cells containing hemoglobin were extruded from the microvessels, subsequently removing the vascular oxygen supply in that area. The PO_2 decrease in that portion of the muscle was proportional to the rate of oxygen consumption by the muscle. Since the initial slope of the line was linear, this indicated that oxygen consumption rate was not dependent on PO_2 at those levels. With a continuous drop in oxygen level, due to continued consumption and no replenishment of oxygen from the blood, the slope of the oxygen disappearance curve decreased until reaching approximately 0 mmHg. The curve in the line indicates a critical point at which the oxygen consumption rate decreased with decreasing PO_2 levels. The time difference from the initial compression to the point where the curve reaches 0 mmHg indicates the total required time for the tissue to consume the oxygen available in the interstitial space. The time it took for that to happen in the SHR and WKY rats ranged from 30-45 seconds.

VO_2 vs. PO_2 Plots

Figures 4 and 5 display the PO_2 dependence of VO_2 plots for a Wistar-Kyoto and Spontaneously Hypertensive Rat, respectively. Hill's equation was used to fit the data to provide a non-linear fit line and key parameters. Vmax indicates the maximum rate of consumption by the tissue in the area being compressed. The PO_2 value at half-maximal consumption rate is represented by P_{50}. A higher P_{50} value is an indication that oxygen consumption rate is oxygen-dependent over a wider range of PO_2 values. On average the SHRs had a higher Vmax compared to the WKY controls.

Explanation for Increased V_{max} in SHRs

The mitochondria are responsible for the consumption of oxygen to produce ATP. One possible explanation for an increased V_{max} in the SHRs could be that there is an inefficiency of oxygen coupling by the mitochondria to produce the normal amount of ATP. In other words, there could be an "uncoupling" of oxygen consumption and ATP production. This could lead to consumption of higher amounts of oxygen to produce the same amount of energy or ATP required for normal cellular processes. In "mitochondrial uncoupling," the electron transport is not used to drive ATP synthesis (Mookerjee SA, 2010). The proton gradient is not efficiently created which compromises the rate at which

ATP is synthesized, hence leading to compensation by an increased rate of respiration. This would explain why oxygen is being consumed at a higher rate as well as the decrease in energy production.

Oxidative Phosphorylation and Glycolysis

In physiologically oxygen-rich environments, the cell produces energy efficiently through oxidative phosphorylation. This fits the classic view of ATP production via oxidative phosphorylation. In anaerobic environments, glycolysis continues to produce lactate independent of oxygen availability. This is suggestive of the fact that mitochondria consume oxygen at a steady rate throughout physiological ranges until the point where PO_2 drops below 1 mmHg. This is a representation of oxidative phosphorylation as the main process producing ATP until PO_2 levels drop to almost zero.

This project used *in vivo* PQM technique to demonstrate that mitochondrial oxygen consumption rate is dependent on PO_2 over a wider physiological range. This rate is dependent on oxygen tension, which indicates that oxidative phosphorylation and glycolysis have to work simultaneously at a rate that is dependent on PO_2. When PO_2 levels are low, the cell can shift to glycolysis for ATP production. Similarly, when the environment is rich in oxygen, the cell can use oxidative phosphorylation. Although this PO_2-dependent ratio of glycolysis and oxidative phosphorylation deviates from the classic view, it is more consistent with oxygen dependence of cellular respiration described in this project and other related studies (Golub AS, Wilson et al).

Limitations and Future Studies

This project did not measure the rate of blood flow in the muscle. It would be beneficial to measure the rate since blood flow is directly related to oxygen delivery to the muscles, and would provide a better understanding of oxygen consumption measurements.

The spinotrapezius muscles used for measurements in this project were at rest. Stimulating a contraction in the muscle could demonstrate how consumption rates are affected in an actively contracted muscle in both healthy and hypertensive rats.

This project used the PQM method with a flash rate of 1 Hz resulting in a PO_2 value per second. The frequency of the laser flash could be increased to provide a better PO_2 resolution of the curves in future studies. This would also in turn, require a correction for the magnitude of photo-consumption by the method. The rats used in this project were age-matched and the approximate age for all the rats was between 10-12 weeks. It would be of interest to compare more “end-stage” hypertensive rats to younger and relatively healthier rats to determine how oxygen consumption differs between rats within the same strain.

Conclusion

In conclusion, the purpose of this project was to determine PO_2 dependence on oxygen consumption, VO_2 in skeletal muscle of spontaneously hypertensive and Wistar-Kyoto control rats. Phosphorescence quenching microscopy was used to measure PO_2 values by arresting blood flow and obtaining an oxygen disappearance curve. The maximum rate of consumption, V_{max} for the SHRs was higher than that of the WKY control rats. Additionally, the P_{50} for the SHR was higher than the WKY controls and indicated that oxygen consumption rate depends on PO_2 over a wide physiological range. It is of importance to further investigate the elevated maximum rate of consumption in the diseased models to understand how hypertension affects cellular respiration and leads to dysfunctional mitochondrial functions.

References

Chance, B., & Williams, G. R. (1956). The respiratory chain and oxidative phosphorylation. *Adv Enzymol Relat Areas Mol Biol*, *17*, 65-134

Costanzo, L.S. (1988). Physiology. Philadelphia, W.B. Saunders Company

Davidman, Morris, and John Opsahl. "Mechanisms of Elevated Blood Pressure in Human Essential Hypertension." *Medical Clinics of North America* 68.2 (1984): 301-20. Web.

Gnaiger, E., Steinlechner- Maran, R., Méndez, G., Eberl, T., & Margreiter, R. (1995). Control of mitochondrial and cellular respiration by oxygen*. Journal of bioenergetics and biomembranes,* 27 (6), 583-596.

Golub, A. S., & Pittman, R. N. (2003). Thermostatic animal platform for intravital microscopy of thin tissues. *Microvascular research*, *66*(3), 213-217

Golub, A. S., & Pittman, R. N. (2012). Oxygen dependence of respiration in rat spinotrapezius muscle in situ. *AJP: Heart and Circulatory Physiology,303*(1). doi:10.1152/ajpheart.00131.2012

Golub, A. S., Tevald, M. A., & Pittman, R. N. (2010). Phosphorescence quenching microrespirometry of skeletal muscle in situ. *AJP: Heart and Circulatory Physiology,300*(1). doi:10.1152/ajpheart.00626.2010

Iuv, Postnov. "Insufficient ATP Production Due to Mitochondrial Calcium Overload as a Source of Blood Pressure Elevation in Primary Hypertension." *PubMed*. N.p., 2005.

Mookerjee SA, Divakaruni AS, Jastroch M, Brand MD. Mitochondrial uncoupling and lifespan. *Mechanisms of ageing and development*. 2010;131(7-8):463-472.

Nugent, W. H., Song, B. K., Pittman, R. N., & Golub, A. S. (2016). Simultaneous sampling of tissue oxygenation and oxygen consumption in skeletal muscle. *Microvascular Research,105*, 15-22.

Nugent, William H., Bjorn K. Song, Roland N. Pittman, and Aleksander S. Golub. "Simultaneous Sampling of Tissue Oxygenation and Oxygen Consumption in Skeletal Muscle." *Microvascular Research* 105 (2016): 15-22. Web.

Nyberg, M., L. Gliemann, and Y. Hellsten. "Vascular Function in Health, Hypertension, and Diabetes: Effect of Physical Activity on Skeletal Muscle Microcirculation." *Scandinavian Journal of Medicine & Science in Sports* 25 (2015): 60-73. Web.

Okamoto, Kozo, and Kyuzo Aoki. "Development of a Strain of Spontaneously Hypertensive Rats." *Japanese Circulation Journal* 27.3 (1963): 282-93. Web.
Pishchany G, Skaar EP. Taste for Blood: Hemoglobin as a Nutrient Source for Pathogens. Heitman J, ed. *PLoS Pathogens*. 2012;8(3)

Pittman, R. N. (2011). *Regulation of tissue oxygenation*. San Rafael, CA: Morgan & Claypool.

Postnov, Yuvenalii V., Sergei N. Orlov, Yegor Y. Budnikov, Alexander D. Doroschuk, and Anton Y. Postnov. "Mitochondrial Energy Conversion Disturbance with Decrease in ATP Production as a Source of Systemic Arterial Hypertension." *Pathophysiology* 14.3-4 (2007): 195-204. *Kardiologiia*.

Smith, T. L., and P. M. Hutchins. "Central Hemodynamics in the Developmental Stage of Spontaneous Hypertension in the Unanesthetized Rat." *Hypertension* 1.5 (1979): 508-17.

Wang, Zuoguang, Xiaoyun Peng, Yongxiang Wei, and Shaojun Wen. "Neglect of Several Important Indexes During the Study of Human Essential Hypertension." *The Journal of Clinical Hypertension* 15.11 (2013): 769-71. Web.

Wells, Rufus M.g. "Chapter 6 Blood- Gas Transport and Hemoglobin Function." *Fish Physiology Hypoxia* (2009): 255-99

Wilson DF, Erecinska M. Effect of oxygen concentration on cellular metabolism. Chest 88: 229S-232S, 1985

Wilson DF, Oxygen pressures in the interstitial space and their relationship to those in the blood plasma in resting skeletal muscle. (2006) J Appl Physiol 101: 1648

Wilson, D. F., Harrison, D. K., & Vinogradov, S. A. (2012). Oxygen, pH, and mitochondrial oxidative phosphorylation. *Journal of Applied Physiology, 113*(12), 1838-1845.

Wilson, D. F., Rumsey, W. L., Green, T. J., & Vanderkooi, J. (1988). The oxygen dependence of mitochondrial oxidative phosphorylation measured by a new optical method for measuring oxygen concentration. *Journal of Biological Chemistry*, *263*(6), 2712-2718.

APPENDIX

VO_2 vs. PO_2 Plots- WKY

A – PO_2 (mmHg)

B – VO_2 (nl O_2/ cm^3 *s)

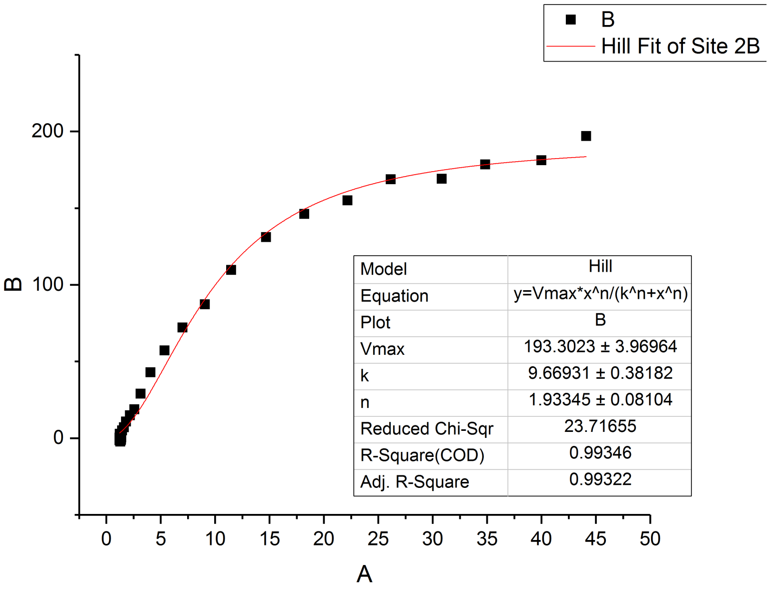

Model	Hill
Equation	y=Vmax*x^n/(k^n+x^n)
Plot	B
Vmax	193.3023 ± 3.96964
k	9.66931 ± 0.38182
n	1.93345 ± 0.08104
Reduced Chi-Sqr	23.71655
R-Square(COD)	0.99346
Adj. R-Square	0.99322

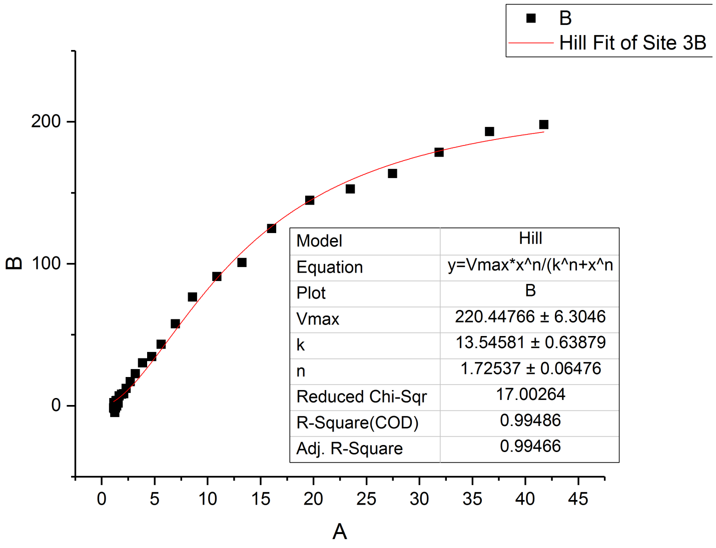

Model	Hill
Equation	y=Vmax*x^n/(k^n+x^n
Plot	B
Vmax	220.44766 ± 6.3046
k	13.54581 ± 0.63879
n	1.72537 ± 0.06476
Reduced Chi-Sqr	17.00264
R-Square(COD)	0.99486
Adj. R-Square	0.99466

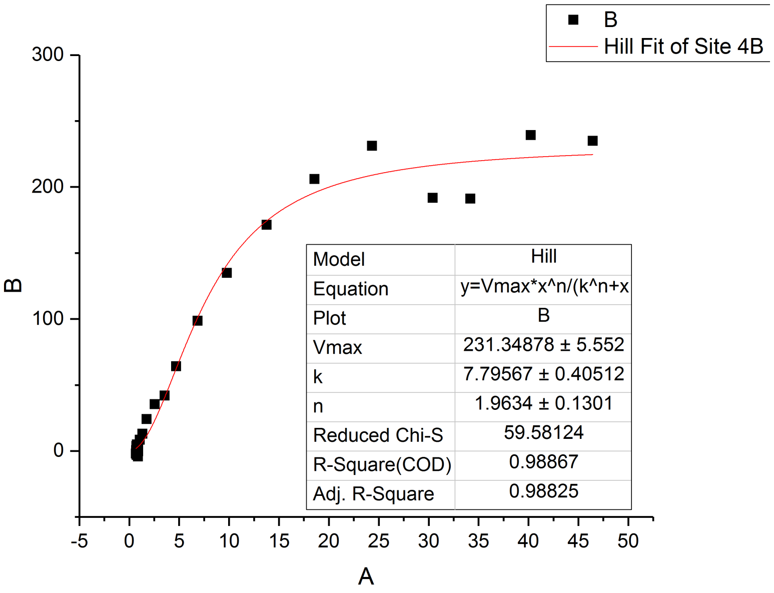

Model	Hill
Equation	y=Vmax*x^n/(k^n+x
Plot	B
Vmax	231.34878 ± 5.552
k	7.79567 ± 0.40512
n	1.9634 ± 0.1301
Reduced Chi-S	59.58124
R-Square(COD)	0.98867
Adj. R-Square	0.98825

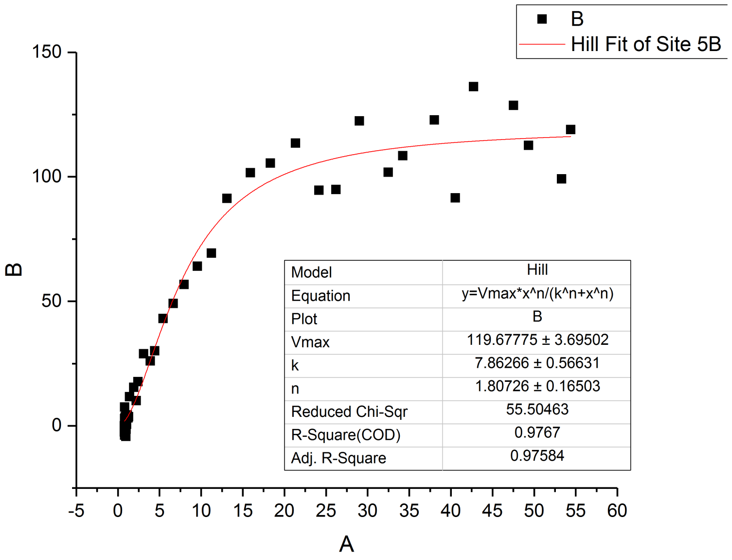

Model	Hill
Equation	y=Vmax*x^n/(k^n+x^n)
Plot	B
Vmax	119.67775 ± 3.69502
k	7.86266 ± 0.56631
n	1.80726 ± 0.16503
Reduced Chi-Sqr	55.50463
R-Square(COD)	0.9767
Adj. R-Square	0.97584

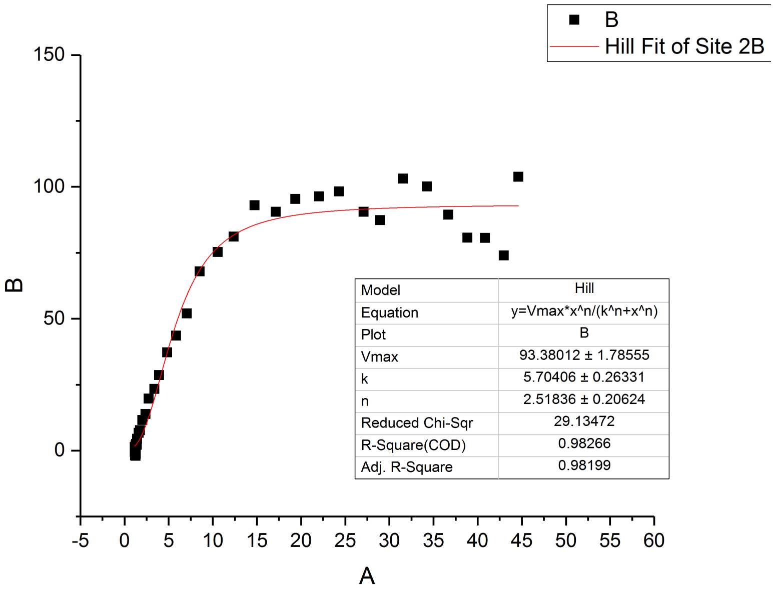

Model	Hill
Equation	y=Vmax*x^n/(k^n+x^n)
Plot	B
Vmax	93.38012 ± 1.78555
k	5.70406 ± 0.26331
n	2.51836 ± 0.20624
Reduced Chi-Sqr	29.13472
R-Square(COD)	0.98266
Adj. R-Square	0.98199

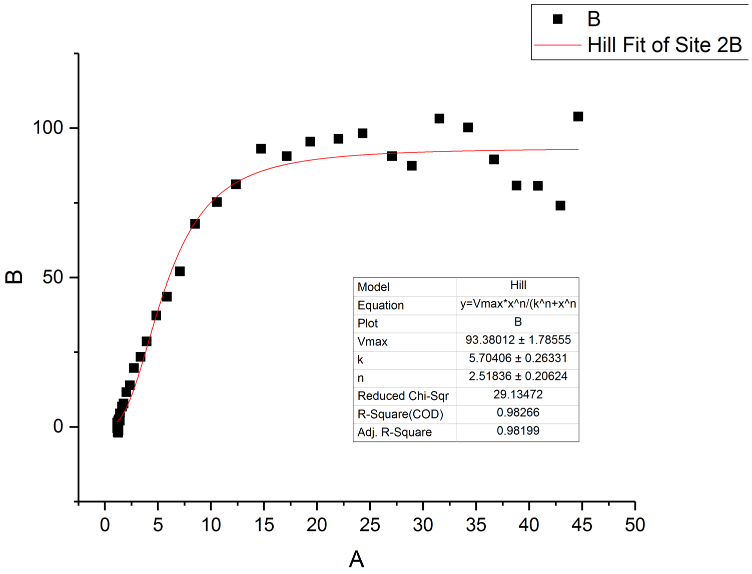

Model	Hill
Equation	y=Vmax*x^n/(k^n+x^n
Plot	B
Vmax	93.38012 ± 1.78555
k	5.70406 ± 0.26331
n	2.51836 ± 0.20624
Reduced Chi-Sqr	29.13472
R-Square(COD)	0.98266
Adj. R-Square	0.98199

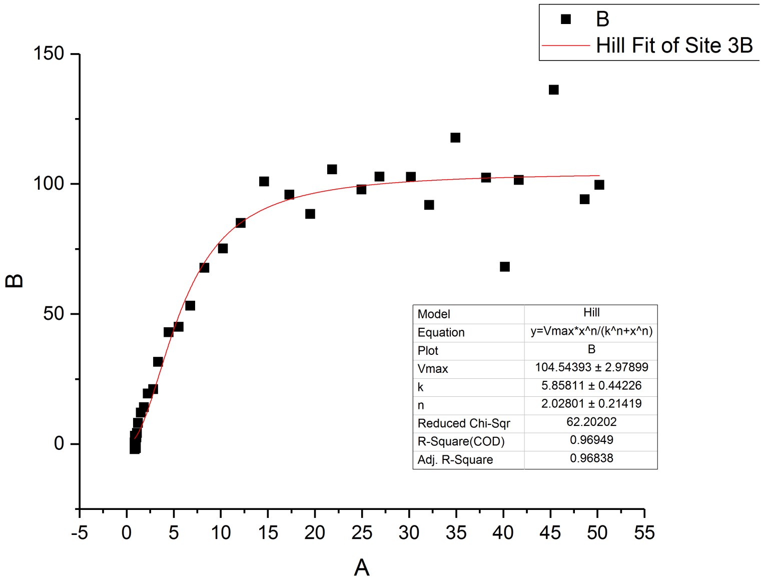

Model	Hill
Equation	y=Vmax*x^n/(k^n+x^n)
Plot	B
Vmax	104.54393 ± 2.97899
k	5.85811 ± 0.44226
n	2.02801 ± 0.21419
Reduced Chi-Sqr	62.20202
R-Square(COD)	0.96949
Adj. R-Square	0.96838

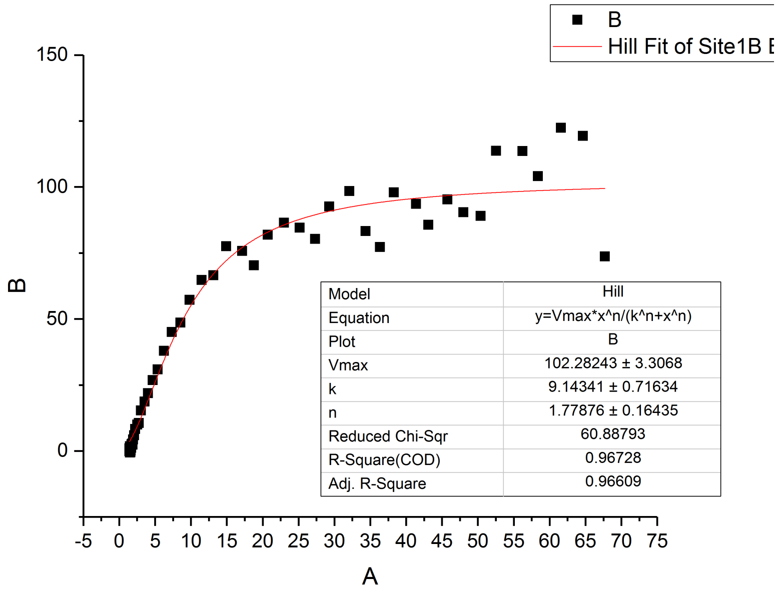

Model	Hill
Equation	y=Vmax*x^n/(k^n+x^n)
Plot	B
Vmax	102.28243 ± 3.3068
k	9.14341 ± 0.71634
n	1.77876 ± 0.16435
Reduced Chi-Sqr	60.88793
R-Square(COD)	0.96728
Adj. R-Square	0.96609

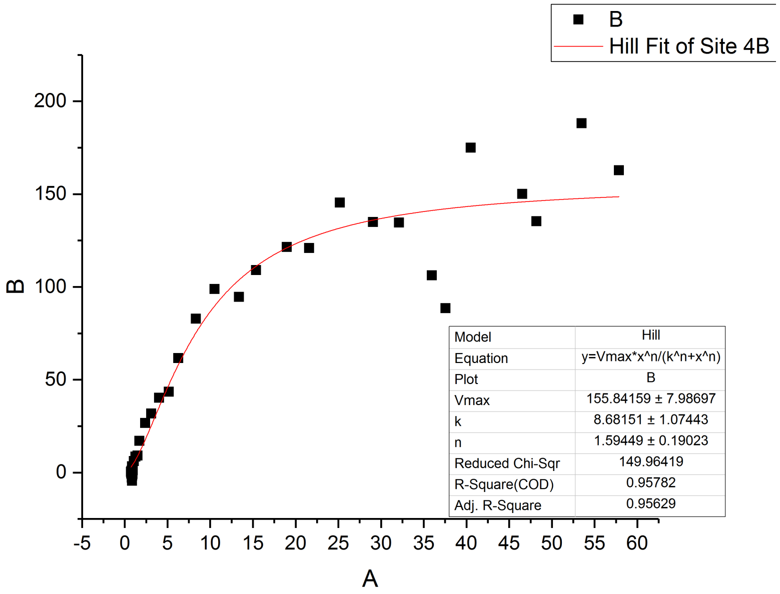

Model	Hill
Equation	y=Vmax*x^n/(k^n+x^n)
Plot	B
Vmax	155.84159 ± 7.98697
k	8.68151 ± 1.07443
n	1.59449 ± 0.19023
Reduced Chi-Sqr	149.96419
R-Square(COD)	0.95782
Adj. R-Square	0.95629

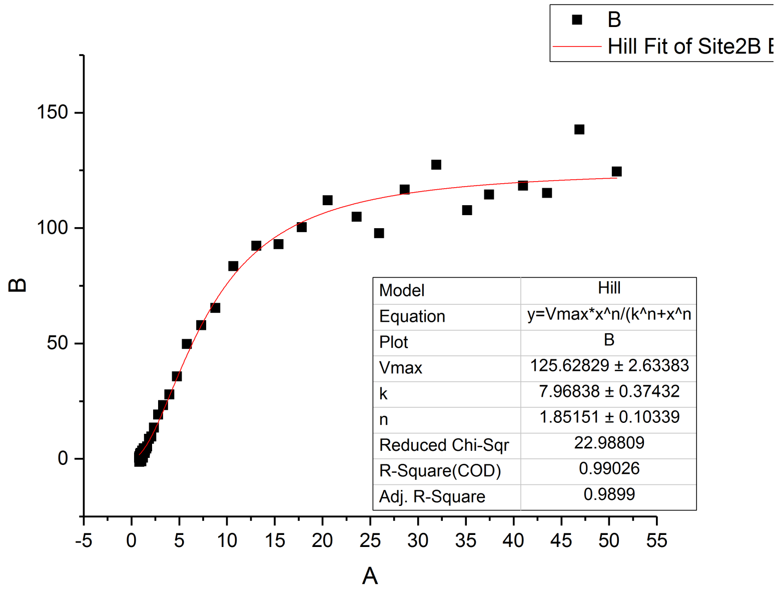

Model	Hill
Equation	y=Vmax*x^n/(k^n+x^n
Plot	B
Vmax	125.62829 ± 2.63383
k	7.96838 ± 0.37432
n	1.85151 ± 0.10339
Reduced Chi-Sqr	22.98809
R-Square(COD)	0.99026
Adj. R-Square	0.9899

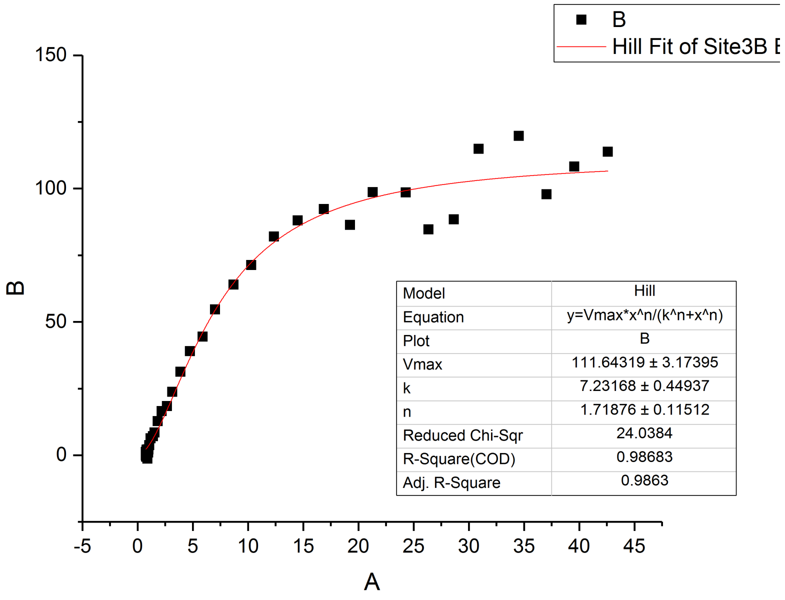

Model	Hill
Equation	y=Vmax*x^n/(k^n+x^n)
Plot	B
Vmax	111.64319 ± 3.17395
k	7.23168 ± 0.44937
n	1.71876 ± 0.11512
Reduced Chi-Sqr	24.0384
R-Square(COD)	0.98683
Adj. R-Square	0.9863

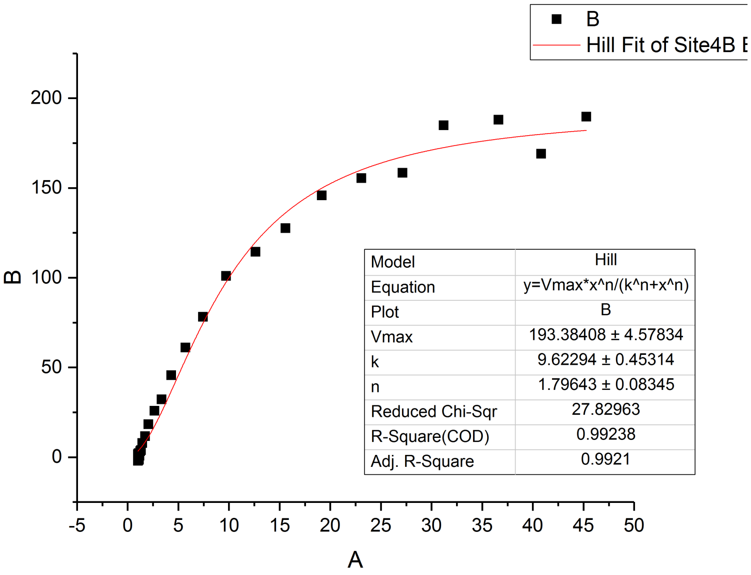

Model	Hill
Equation	y=Vmax*x^n/(k^n+x^n)
Plot	B
Vmax	193.38408 ± 4.57834
k	9.62294 ± 0.45314
n	1.79643 ± 0.08345
Reduced Chi-Sqr	27.82963
R-Square(COD)	0.99238
Adj. R-Square	0.9921

VO_2 vs. PO_2 Plots- SHR

A – PO_2 (mmHg)

B – VO_2 (nl O_2/ cm^3 *s)

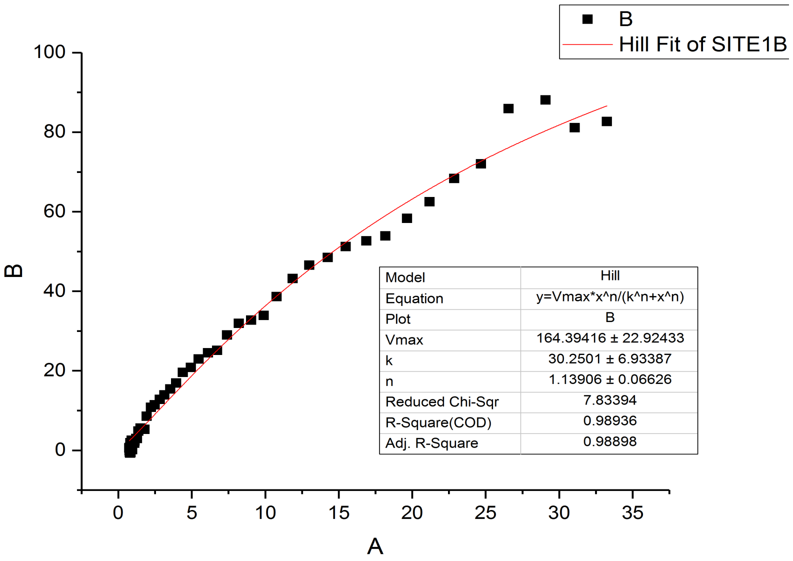

Model	Hill
Equation	y=Vmax*x^n/(k^n+x^n)
Plot	B
Vmax	164.39416 ± 22.92433
k	30.2501 ± 6.93387
n	1.13906 ± 0.06626
Reduced Chi-Sqr	7.83394
R-Square(COD)	0.98936
Adj. R-Square	0.98898

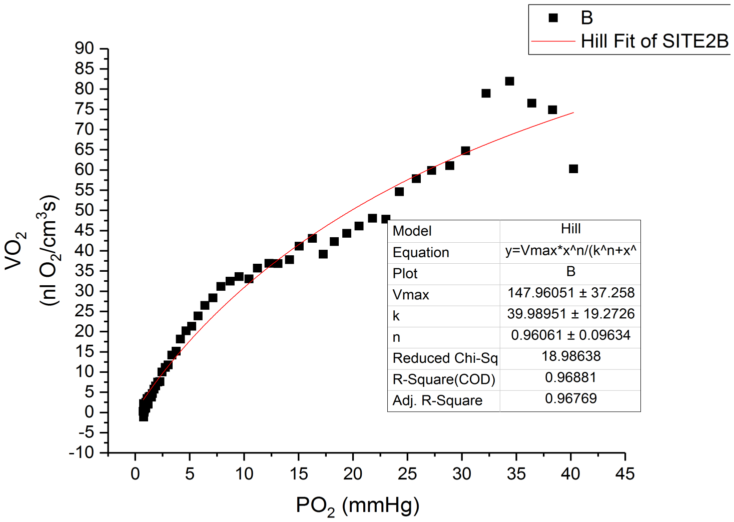
B
Hill Fit of SITE2B
Model | Hill
Equation | y=Vmax*x^n/(k^n+x^
Plot | B
Vmax | 147.96051 ± 37.258
k | 39.98951 ± 19.2726
n | 0.96061 ± 0.09634
Reduced Chi-Sq | 18.98638
R-Square(COD) | 0.96881
Adj. R-Square | 0.96769
VO2 (nl O2/cm3s)
90
85
80
75
70
65
60
55
50
45
40
35
30
25
20
15
10
5
0
-5
-10
0
5
10
15
20
25
30
35
40
45
PO2 (mmHg)

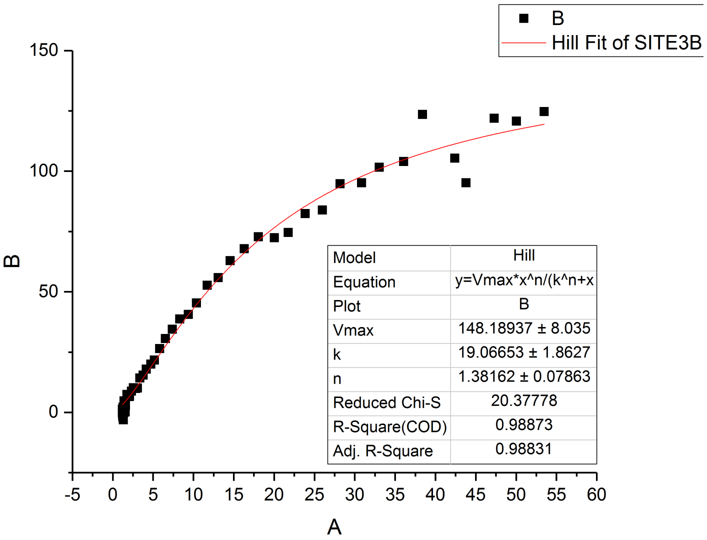
B
Hill Fit of SITE3B
Model | Hill
Equation | y=Vmax*x^n/(k^n+x
Plot | B
Vmax | 148.18937 ± 8.035
k | 19.06653 ± 1.8627
n | 1.38162 ± 0.07863
Reduced Chi-S | 20.37778
R-Square(COD) | 0.98873
Adj. R-Square | 0.98831
B
150
100
50
0
-5
0
5
10
15
20
25
30
35
40
45
50
55
60
A

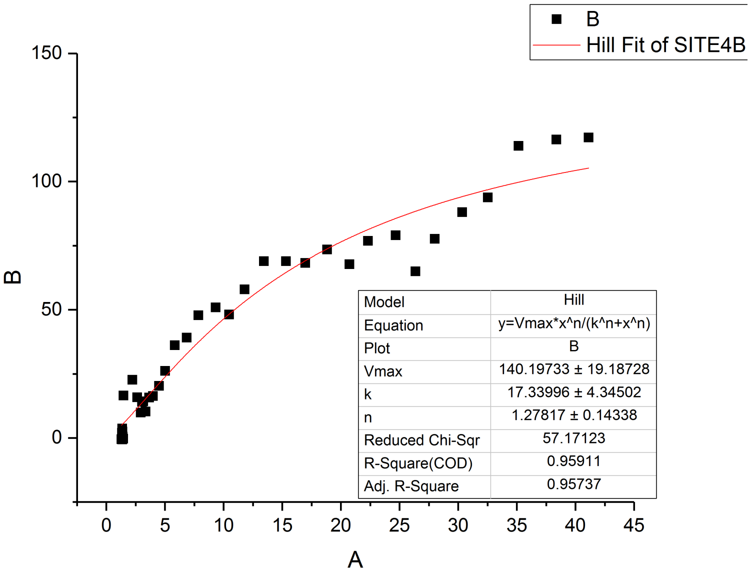

Model	Hill
Equation	y=Vmax*x^n/(k^n+x^n)
Plot	B
Vmax	140.19733 ± 19.18728
k	17.33996 ± 4.34502
n	1.27817 ± 0.14338
Reduced Chi-Sqr	57.17123
R-Square(COD)	0.95911
Adj. R-Square	0.95737

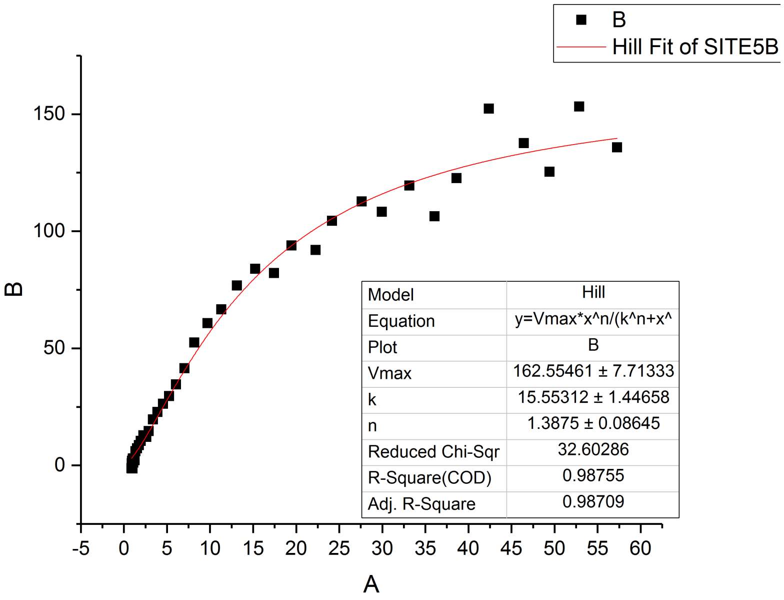

Model	Hill
Equation	y=Vmax*x^n/(k^n+x^
Plot	B
Vmax	162.55461 ± 7.71333
k	15.55312 ± 1.44658
n	1.3875 ± 0.08645
Reduced Chi-Sqr	32.60286
R-Square(COD)	0.98755
Adj. R-Square	0.98709

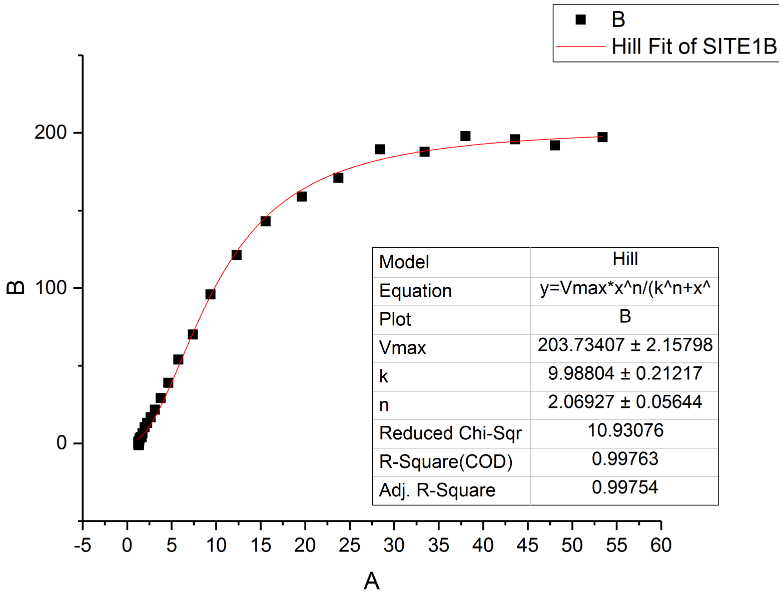

Model	Hill
Equation	y=Vmax*x^n/(k^n+x^
Plot	B
Vmax	203.73407 ± 2.15798
k	9.98804 ± 0.21217
n	2.06927 ± 0.05644
Reduced Chi-Sqr	10.93076
R-Square(COD)	0.99763
Adj. R-Square	0.99754

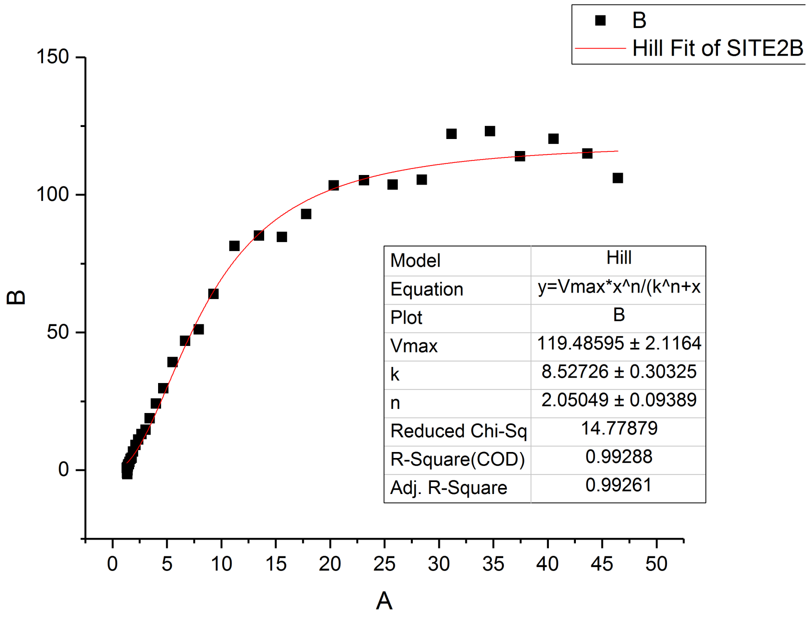

Model	Hill
Equation	y=Vmax*x^n/(k^n+x
Plot	B
Vmax	119.48595 ± 2.1164
k	8.52726 ± 0.30325
n	2.05049 ± 0.09389
Reduced Chi-Sq	14.77879
R-Square(COD)	0.99288
Adj. R-Square	0.99261

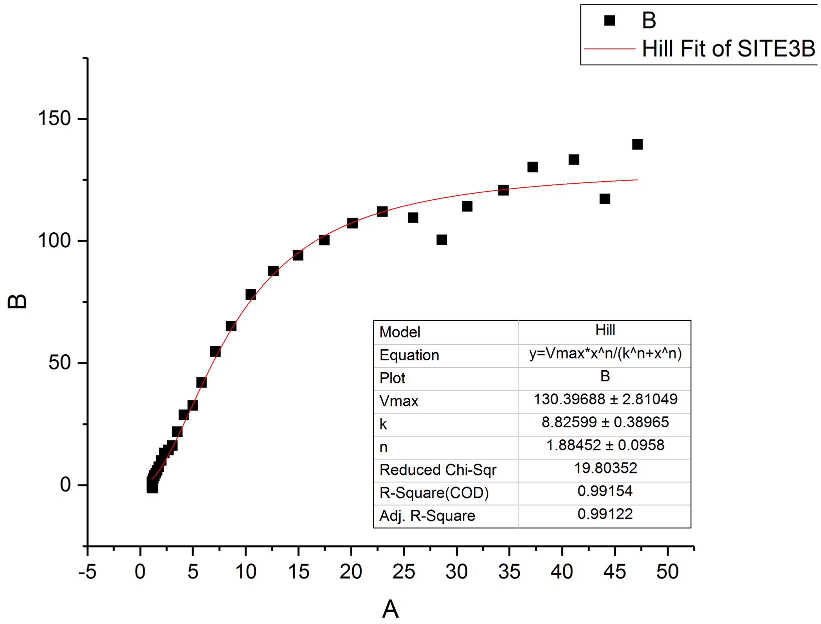

Model	Hill
Equation	y=Vmax*x^n/(k^n+x^n)
Plot	B
Vmax	130.39688 ± 2.81049
k	8.82599 ± 0.38965
n	1.88452 ± 0.0958
Reduced Chi-Sqr	19.80352
R-Square(COD)	0.99154
Adj. R-Square	0.99122

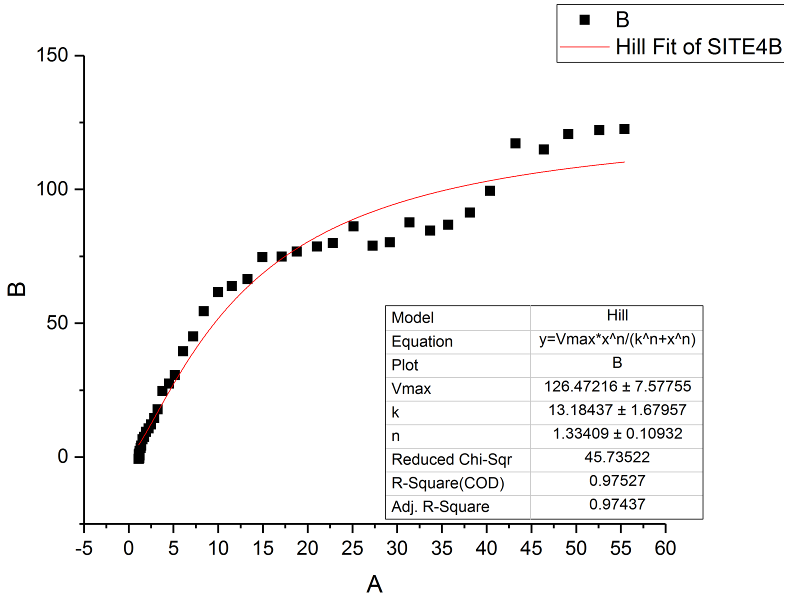

Model	Hill
Equation	y=Vmax*x^n/(k^n+x^n)
Plot	B
Vmax	126.47216 ± 7.57755
k	13.18437 ± 1.67957
n	1.33409 ± 0.10932
Reduced Chi-Sqr	45.73522
R-Square(COD)	0.97527
Adj. R-Square	0.97437

VITA

Habiba Shah was born in Peshawar, Pakistan on July 1^{st}, 1991. She moved to the United States in October 2006 and graduated from George Washington High School in Danville, Virginia in June 2009. She received her Bachelor of Science degree in Forensic Science from Virginia Commonwealth University in December 2013. She went on to pursue a Master of Science degree in Physiology and Biophysics at the VCU School of Medicine in August 2017.